

812. Effective reduction of stiffness at peak frequency in hydraulic engine mounts by using magneto-rheological fluids

Reza Tikani¹, Saeed Ziaei-Rad², Nader Vahdati³

^{1,2}Department of Mechanical Engineering, Isfahan University of Technology, Isfahan 84156-83111, Iran

³Mechanical Engineering Department, Petroleum Institute, P. O. Box 2533, Abu Dhabi, UAE

E-mail: ¹r_tikani@cc.iut.ac.ir, ²szrad@cc.iut.ac.ir, ³nvahdati@pi.ac.ae

(Received 14 April 2012; accepted 14 May 2012)

Abstract. Hydraulic engine mounts are generally used in aerospace and automotive applications for the purpose of cabin noise and vibration reduction. By careful selection of hydraulic mount design parameters, at a certain frequency, namely the notch frequency, the dynamic stiffness will be smaller than the static stiffness and cabin vibration and noise reduction is provided at that frequency. Literature review indicates that in all previous designs of hydraulic engine mounts the dynamic stiffness increases after the notch frequency. This phenomenon is undesirable because of the increase in the force transmitted to the cabin. This paper proposes a new hydraulic engine mount that uses two working fluids. The new design has two notch frequencies and two peak frequencies. In this study, effective reduction of the peak frequencies has been demonstrated by using a controllable fluid as one of the working fluids and a non-controllable fluid as the second working fluid. As a result, one can obtain a hydraulic engine mount design with only one notch frequency but having no peak frequency. The new hydraulic engine mount design and its mathematical model are presented in detail and some discussions on the simulation results are provided.

Keywords: hydraulic engine mount, fluid mount, magneto-rheological fluid, peak frequency, vibration reduction, NVH.

Nomenclature

V_m	Velocity across the mount
A_p	Effective piston area of the mount, top chamber
A_i	Cross-section area of the inner rubber
I_f	Fluid inertia in the inertia track
R_f	Inertia track flow resistance
K_r	Axial stiffness of the top rubber
B_r	Damping component of the top rubber
K_v	Chamber volumetric stiffness
m	Inner top metal weight
K	Stiffness of spring between outer and inner mount
L	Inertia track length
D	Inertia track diameter
g	Radial gap in the inner mount
ρ	Fluid density
μ	Fluid dynamic viscosity

ω	Circular frequency
S	Equal to $j\omega$
q_2	Relative motion across the mount
q_6	Top chamber change in volume (outer mount)
q_{10}	Bottom chamber change in volume (outer mount)
q_{12}	Relative motion across the spring
q_{18}	Relative motion across the inner mount
q_{21}	Top chamber change in volume (inner mount)
q_{24}	Bottom chamber change in volume (inner mount)
P_8	Time integral of the pressure drop in the outer inertia track (pressure momentum)
P_{16}	Inner rubber top metal momentum
P_{23}	Time integral of the pressure drop in the inner inertia track (pressure momentum)
ΔP_{MR}	Pressure drop in the inner inertia track
I	Electric current
H	Magnetic field intensity
τ	MR-fluid yield strength

Subscripts

o	Outer mount
i	Inner mount
t	Top chamber
b	Bottom chamber

Introduction

Hydraulic engine mounts are generally used to connect two structures together and to reduce vibration transmission from one to the other. Hydraulic engine mounts or fluid mounts are elastomeric mounts with fluid traveling between the top and bottom compliant fluid chambers, see Fig. 1 [1]. A fluid channel between the two chambers, called "inertia track", is used to connect them together [2]. Depending on the mount parameters, the resonance caused by the oscillating fluid in the inertia track can either provide additional damping to the fundamental mount resonance (using a high viscosity fluid) [3], or create a tuned vibration absorber effect (using a low viscosity fluid) [4] to provide vibration isolation at a particular frequency called notch frequency. This paper focuses on the latter.

A single-pumper [4] or a single acting passive hydraulic (or fluid) engine mount, as shown in Fig. 1, consists of two fluid chambers that are connected together via an inertia track. Fig. 2 indicates that the dynamic stiffness is the lowest at a frequency referred to as notch frequency. Its location depends on the inertia track length, diameter, fluid density, and rubber stiffness. Fig. 2 shows a typical dynamic stiffness of a passive hydraulic engine mount versus frequency.

At the notch frequency, the dynamic stiffness will be smaller than the static stiffness and cabin noise and vibration reduction is the highest at that frequency. One of the shortcomings of the hydraulic engine mounts is the peak frequency (see Fig. 2). The peak corresponds to the

resonance frequency of the slug of the fluid that is flowing back and forth in the inertia track, bouncing against the bulge or volumetric stiffness of the top and bottom elastomeric chambers. Near and at the notch frequency, excellent cabin noise and vibration reduction is achieved due to the mount dynamic stiffness being low, but near the peak frequency, due to increase in hydraulic mount dynamic stiffness, cabin noise and vibration is the worst. To overcome this drawback, researchers have focused on active hydraulic engine mounts [5-7] to control the mount dynamic stiffness beyond the notch frequency. Producing a reliable active engine mount is difficult since it requires an actuator, a controller, a software, adequate sealing, moving parts, and large amounts of energy to run the actuator and the controller.

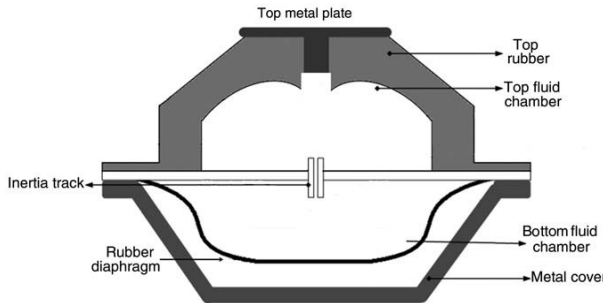


Fig. 1. A typical single pumper hydraulic engine mount

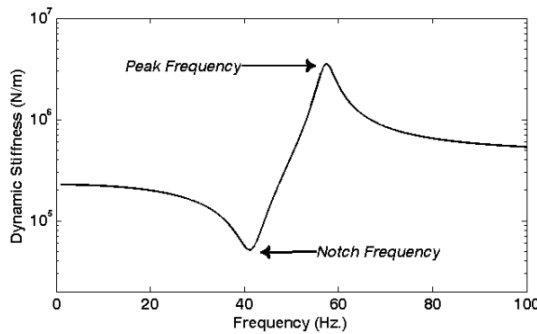


Fig. 2. Dynamic stiffness of a typical hydraulic engine mount

Semi-active engine mounts especially magneto-rheological hydraulic mounts have the ability of real-time control of the mount dynamic properties [8]. An extensive literature review was conducted by the authors to find semi-active hydraulic engine mount designs that have capability of eliminating or reducing the dynamic stiffness at the peak frequency without any effect on the notch depth. Ahmadian and Ahn [5] proposed a hydraulic engine mount that used magneto-rheological fluids (MR fluids) as the working fluid and an MR valve was used to control damping. The peak frequency of their MR-fluid hydraulic engine mount design was eliminated by turning on the magnetic field, when the frequency sweep approached the peak frequency. The magnetic field was not active all the time but only when the frequency sweep approached the peak frequency. If the MR-valve is turned on at all times, the high frequency dynamic stiffness is improved but at the expense of low frequency dynamic stiffness. In the design presented in this paper, the peak frequency elimination has been achieved but not at the expense of the notch frequency degradation.

In aerospace applications, at the cruise speed, there are many imbalance (disturbance) excitation frequencies [9] and ideally one wants to isolate the cabin from all engine imbalance

excitation frequencies. However, with the current hydraulic engine mount technology, the hydraulic mount notch frequency can only be tuned to one and only one frequency. For example, in most turbofan engines, the largest imbalance excitation amplitudes normally occur at N_1 (engine low-speed shaft imbalance excitation frequency) and at N_2 frequencies (engine high-speed shaft imbalance excitation frequency). Since the current hydraulic engine mount design technology only offers isolation at one frequency, a hydraulic mount designer has no choice but to select isolation at N_1 or at N_2 [10] but not at both.

Literature and patent review show that Vahdati [10] has worked on passive hydraulic engine mount designs that can provide vibration and noise isolation at two distinct frequencies. In his design, instead of conventional two fluid chambers, three fluid chambers and two inertia tracks were used to create a double notch fluid mount design.

Another passive hydraulic engine mount design with two notch frequency is reported by Tikani et al. [11]. In this design, two distinct notch frequencies can be obtained by using two working fluids. By using a high viscosity fluid in the inner mount of this design, it can be converted to a hydraulic engine mount with only one notch frequency without any peak frequency.

Here in this paper, the aforementioned design is improved by using a magneto-rheological fluid to obtain a semi-active hydraulic engine mount. In the absence of applied current, this mount has two notch frequencies and two peak frequencies. By applying the current to the magnetic coil, magnetic field will be produced leading to increase of flow resistance of magneto-rheological fluid in the inner mount. In this condition a new behavior takes place and a hydraulic engine mount with only one notch frequency and without peak frequency will be obtained. This design can be applied in aerospace industry (turbofan engines) as well as automotive industry (variable displacement engines) to reduce the transmitted vibration to the cabin. By using control strategies one can reduce the engine vibration by changing the applied current to the mount.

The new hydraulic engine mount design and its mathematical model are presented in detail and some discussions on the simulation results are also included.

Double-notch passive hydraulic engine mount

In the previous section, it was mentioned that with a single-notch hydraulic engine mount design, cabin noise and vibration reduction can only be possible at one frequency (at the notch frequency). Here in this section, a double-notch passive hydraulic engine mount design concept will be described, that can filter out two imbalance disturbance inputs from the cabin.

Fig. 3 shows the new double-notch hydraulic engine mount design concept. It is based on two complete single pumper hydraulic engine mounts (one inside the other). The two hydraulic engine mounts (the inner one and the outer one) are completely independent from each other and the only interaction between the two is through a spring and a fabric diaphragm. In this new design, two independent top chambers are connected with inertia tracks to the bottom chambers. The outer mount is filled with a low viscosity fluid and the inner mount is filled with a magneto-rheological fluid.

The outer and the inner rubbers, which are custom-designed rubber components, act like a spring in the axial direction, act like a piston pumping fluid, and act like a volumetric spring in the volumetric or bulge direction containing the fluid. In the outer and the inner bottom fluid chambers, a soft rubber diaphragm provides the volumetric stiffness and contains the fluid. Fig. 4 illustrates the schematics of the mount including major parameters.

The bond graph model in the absence of input current to the electromagnetic coil is shown in Fig. 5. In mechanical domain, effort and flow can be identified as force and velocity. In the hydraulic domain, these variables are total pressure and volume flow rate, respectively.

The state space equations, from the bond graph model of Fig. 5, can be derived as follows:

$$\dot{q}_2 = V_{in} \tag{1}$$

$$\dot{q}_6 = A_{po} V_{in} - \frac{P_8}{I_8} - A_i \frac{P_{16}}{I_{16}} \tag{2}$$

$$\dot{P}_8 = \frac{q_6}{C_6} - R_9 \frac{P_8}{I_8} - \frac{q_{10}}{C_{10}} \tag{3}$$

$$\dot{q}_{10} = \frac{P_8}{I_8} \tag{4}$$

$$\dot{q}_{12} = V_{in} - \frac{P_{16}}{I_{16}} \tag{5}$$

$$\dot{P}_{16} = A_i \frac{q_6}{C_6} + \frac{q_{12}}{C_{12}} - R_{17} \frac{P_{16}}{I_{16}} - \frac{q_{18}}{C_{18}} - A_{pi} \frac{q_{21}}{C_{21}} \tag{6}$$

$$\dot{q}_{18} = \frac{P_{16}}{I_{16}} \tag{7}$$

$$\dot{q}_{21} = A_{pi} \frac{P_{16}}{I_{16}} - \frac{P_{23}}{I_{23}} \tag{8}$$

$$\dot{P}_{23} = \frac{q_{21}}{C_{21}} - R_{25} \frac{P_{23}}{I_{23}} - \frac{q_{24}}{C_{24}} \tag{9}$$

$$\dot{q}_{24} = \frac{P_{23}}{I_{23}} \tag{10}$$

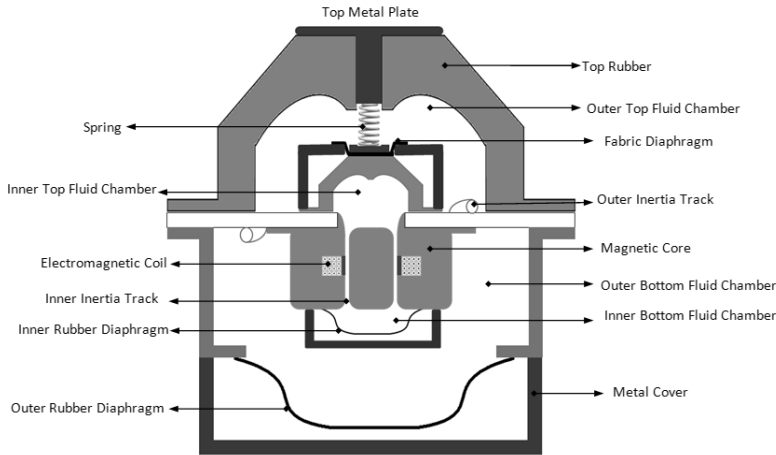


Fig. 3. Double-notch hydraulic engine mount

The input force (effort on bond 1) is given by:

$$F_{in} = \frac{q_2}{C_2} + R_3 V_{in} + A_{po} \frac{q_6}{C_6} + \frac{q_{12}}{C_{12}} \tag{11}$$

In the above state space equations $q_2, q_6, q_{10}, q_{12}, q_{18}, q_{21}$ and q_{24} are the generalized displacement variables (time integral of flows), and P_8, P_{16} and P_{23} are the momentum variables (time integral of efforts).

$$\begin{aligned}
 \lambda_1 &= s^2 I_8 + R_9 s + \frac{1}{C_{10}} \\
 \lambda_2 &= s^2 I_{23} + R_{25} s + \frac{1}{C_{24}} \\
 \lambda_3 &= s^2 I_{16} + R_{17} s + \frac{1}{C_{18}} \\
 \gamma &= \lambda_3 + \frac{A_i^2}{C_6 + \frac{1}{\lambda_1}} + \frac{A_{pi}^2}{C_{21} + \frac{1}{\lambda_2}}
 \end{aligned}
 \tag{13}$$

The lowest dynamic stiffness (occurring at the notch frequencies) occurs when the numerator of Eqn. (12) is set to zero, and the maximum dynamic stiffness (occurring at the peak frequencies) occurs when the denominator is set to zero. It was shown in [10] that the notch and the peak frequency locations are weakly sensitive to damping. So one can find the notch and the peak frequencies by setting all the damping factors to zero.

To simulate the model in Fig. 5, MATLAB program and the above state space equations with the baseline parameters described in Table 1 were used.

Table 1. Numerical values of the parameters for the proposed hydraulic engine mount

Symbol	Value	Units
A_{po}	0.0077	m ²
A_{pi}	0.0017	m ²
A_i	0.0036	m ²
$K_{ro} (= 1/C_2)$	$3.25 \cdot 10^6$	N/m
$K_{ri} (= 1/C_{18})$	$2.6 \cdot 10^6$	N/m
$K_{vto} (= 1/C_6)$	$3.34 \cdot 10^{11}$	N/m ⁵
$K_{vbo} (= 1/C_{10})$	$6.69 \cdot 10^9$	N/m ⁵
$K_{vri} (= 1/C_{21})$	$2.38 \cdot 10^{11}$	N/m ⁵
$K_{vbi} (= 1/C_{24})$	$4.77 \cdot 10^9$	N/m ⁵
$K (= 1/C_{12})$	$1 \cdot 10^3$	N/m
$B_{ro} (= R_3)$	258	Ns/m
$B_{ri} (= R_{17})$	217	Ns/m
$R_{fo} (= R_9)$	$1.94 \cdot 10^4$	Ns/m ⁵
$R_{fi} (= R_{25})$	$5.60 \cdot 10^6$	Ns/m ⁵
$m (= I_{16})$	0.05	kg
L_o	0.1	m
L_i	0.06	m
D_o	0.018	m
D_i	0.03	m
g	0.004	m
ρ_o	760	kg/m ³
ρ_{MR}	2400	kg/m ³
μ_o	$0.5 \cdot 10^{-3}$	Pa·s
μ_{MR}	0.061	Pa·s

In this paper, the flow in the inertia track is assumed to be laminar so the fluid inertia, in each inertia track, is given by [12]:

$$I_f = \frac{4\rho L}{\pi D^2} \quad (14)$$

The resistance of the outer inertia track with circular cross-section can be expressed as [12]:

$$R_{fo} = \frac{128\mu L_o}{\pi D^4} \quad (15)$$

The resistance of the inner inertia track, which is an annular section, is given as follows [12]:

$$R_{fi} = \frac{8\mu L_i}{\pi D_i g^3 \left(1 - \frac{g}{D_i}\right)} \quad (16)$$

With the above baseline parameters, MATLAB program was used to simulate the state space Eqns. (1)-(11). Fig. 6 shows the new hydraulic engine mount dynamic stiffness versus frequency with two notches and two peaks. It illustrates that the first and the second notch frequencies occur at 61.3 and 123.4 Hz, respectively, and the peak frequencies at 96.1 and 142.2 Hz, respectively. Figs. 7-8 are the magnified version of Fig. 6, but zoomed to the two notches.

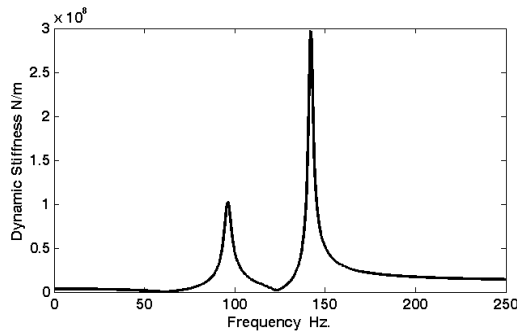


Fig. 6. Dynamic stiffness of double notch hydraulic mount (MATLAB simulation)

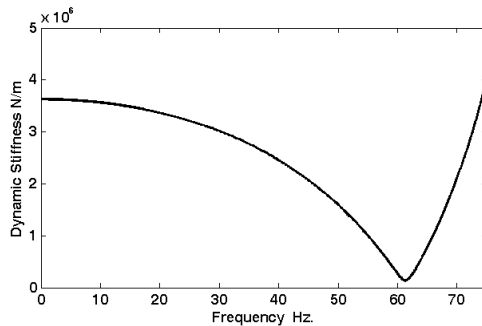


Fig. 7. First notch frequency of the proposed hydraulic mount

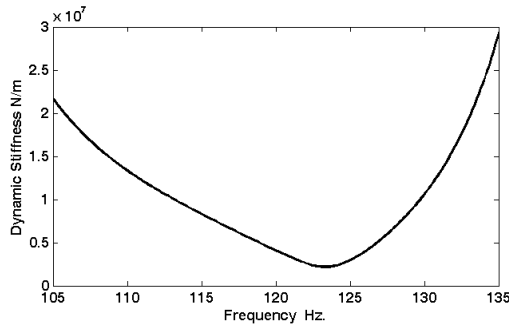


Fig. 8. Second notch frequency of the proposed hydraulic mount

By choosing very high axial stiffness of the inner mount the hydraulic engine mount will be converted to the simple engine mount and one can check the validity of the solution by comparing the dynamic stiffness of the mount with that of the simple hydraulic engine mount [13].

It is important to note that one can put the notch and peak frequencies to desired locations by effectively choosing appropriate hydraulic engine mount parameters. To show which mount parameters have the most influence on the location of the notch and peak frequencies, a sensitivity analysis has been conducted. In this analysis, each parameter of the hydraulic engine mount is varied by 20 % and the percentage change on the location of the notch and the peak frequencies are then calculated. The obtained results are listed in Table 2.

Table 2. The sensitivity of the notch and the peak frequencies to 20 % change in the mount parameters

Baseline Parameters	Change in First Notch Frequency 61.3 Hz	Change in Second Notch Frequency 123.4 Hz	Change in First Peak Frequency 96.1 Hz	Change in Second Peak Frequency 142.2 Hz
$K_{ro} = 3.25e6$	5.3 %	0.4 %	0.0 %	0.0 %
$K_{ri} = 2.6e6$	1.6 %	1.2 %	5.6 %	0.1 %
$A_{po} = 0.0077$	-10.3 %	-0.7 %	0.0 %	0.0 %
$D_o = 0.018$	19.5 %	0.3 %	10.4 %	8.4 %
$L_o = 0.1$	-8.3 %	-0.1 %	-7.1 %	-1.7 %
$A_{pi} = 0.0017$	-0.2 %	-3.4 %	-2.6 %	0.8 %
$D_i = 0.03$	0.1 %	8.9 %	3.0 %	5.7 %
$L_i = 0.06$	-0.1 %	-8.9 %	-3.8 %	-5.9 %
$K_{vto} = 3.34e11$	0.9 %	0.1 %	2.0 %	1.6 %
$K_{vti} = 2.38e11$	0.0 %	7.5 %	0.8 %	7.6 %
$K_{vbo} = 6.60e9$	1.5 %	0.0 %	0.5 %	0.1 %
$K_{vbi} = 4.77e9$	0.0 %	0.3 %	0.1 %	0.2 %
$A_i = 0.0036$	-3.4 %	0.8 %	-9.3 %	-0.7 %
$g = 0.004$	0.1 %	10.5 %	3.1 %	7.7 %

The results indicate that the first notch frequency has high sensitivity to the outer inertia track parameters, i.e. diameter, length, and the effective piston area of the outer mount. The inner mount inertia parameters (gap size, diameter and length) plus the top volumetric stiffness of the inner mount are the most effective parameters on the second notch frequency location. The first peak frequency is the most sensitive to the outer inertia track parameters meaning diameter, length, and cross-section area of the inner mount rubber. The outer inertia track diameter, the inner inertia track length, diameter and gap size, and the volumetric stiffness of the inner top chamber have the greatest effect on the second peak frequency.

Sometimes it is necessary to alter the location of the notch frequencies after the fluid mount is manufactured. Retuning the notch frequencies location can be done without a need for any fluid mount redesign by using gas pressure behind the rubber in the bottom chambers. The details can be found in [10].

Figs. 9 and 10 show the variation in the dynamic stiffness as a function of the outer inertia track diameter. The effective change in the first notch frequency can be easily observed in Fig. 10. The second notch frequency does not change by altering this parameter.

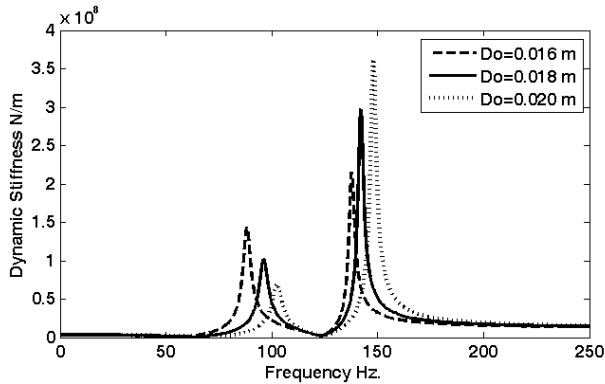


Fig. 9. Dynamic stiffness of the hydraulic mount by altering the outer inertia track diameter

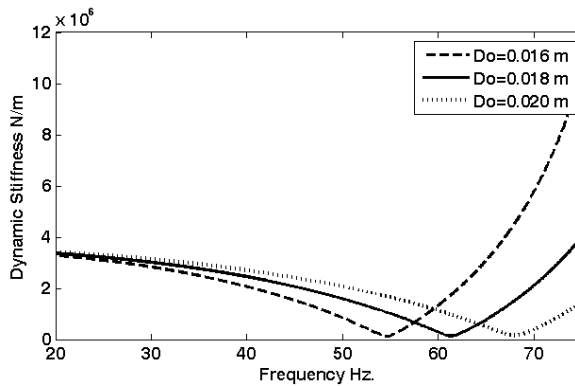


Fig. 10. Change in the first notch frequency by altering the outer inertia track diameter

Fig. 11 illustrates the change in the dynamic stiffness by altering the radial gap in the inner mount. The first notch frequency does not change, but the other dynamic stiffness properties change by altering this parameter. Fig. 12 demonstrates the effect of variation of inner rubber cross-section area on the dynamic stiffness. This parameter can alter the first peak location, effectively.

Magnetic field effect

As it was shown in Fig. 3, the MR-fluid will be used in the most inner mount. By applying the magnetic field to the inner mount, the pressure drop in the inner inertia track will be increased and the dynamic stiffness properties will be varied.

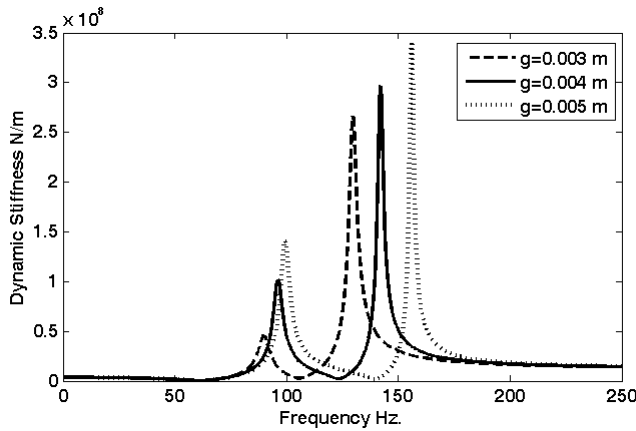


Fig. 11. Dynamic stiffness of the hydraulic mount by altering the radial gap of the inner mount

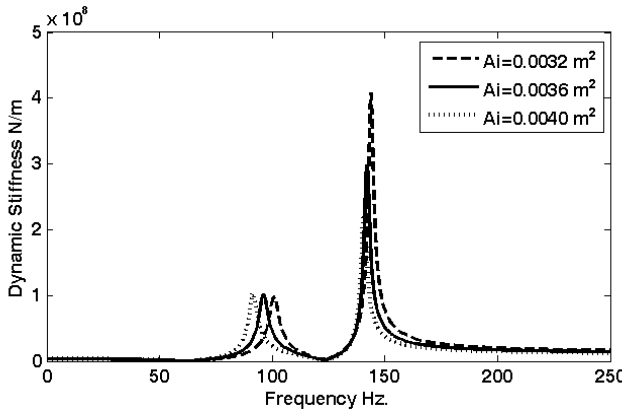


Fig. 12. Dynamic stiffness of the hydraulic mount by altering the inner rubber cross section area

Considering the pressure drop in the inner inertia track due to the application of the magnetic field, Eqn. (9) can be written as:

$$\dot{P}_{23} = \frac{q_{21}}{C_{21}} - R_{25} \frac{P_{23}}{I_{23}} - \frac{q_{24}}{C_{24}} - \Delta P_{MR} \text{sign}(P_{23}) \quad (17)$$

where ΔP_{MR} is the pressure drop in the inner inertia track. According to [14], the pressure difference caused by the magneto-rheological effect can be expressed as:

$$\Delta P_{MR} = \frac{c\tau(H)L_t}{g} \quad (18)$$

The parameter c in the Eqn. (18) is a constant in the range of 2 to 3, depending on the steady-state flow conditions. In this study, corresponding to low flow conditions, it is assumed that c is equal to 2. The MR fluid yield strength, which is magnetic field (H) dependent, is displayed by $\tau(H)$ in Eqn. (18).

Barber and Carlson [15] introduced an empirical equation between MR-fluid yield strength containing 22 % iron, $\tau(H)$, and the applied magnetic field, H , as follows:

$$\tau(H) = 2.704 \times 10^4 \tanh(6.33 \times 10^{-6} H) \quad (19)$$

The applied magnetic field can be calculated based on the simplified Kirchhoff's law for magnetic circuits [16]:

$$H = \frac{N_c I}{2g} \quad (20)$$

here, N_c is the turn number of the coil winding in the inner mount and I is the current input. A cylindrical coil made of 400 turns with the maximum current up to 1.4 A was considered. By using Eqns. (19) and (20) the yield strength of the MR fluid can be obtained and one can calculate the pressure drop, from Eqn. (18), due to application of the magnetic field.

Dynamic stiffness of hydraulic engine mount in the on-state mode

Fig. 13 presents the dynamic stiffness of the hydraulic engine mount in the ON (0.4 Amp.) and OFF states. By applying different current values to the electromagnetic coil, the pressure drop in the inner inertia track can be varied and thus one can generate the desired dynamic stiffness curve. Also, in special conditions, as shown in Fig. 13, the peak frequency can be eliminated. Fig. 14 provides different dynamic stiffness curves that can be obtained by changing the magnetic field. Increase in the input current will cause higher magnetic field through the MR fluid. By increasing the magnetic field the first and the second peak frequencies in the dynamic stiffness decrease, whereas the first notch frequency depth does not change much (Fig. 15). More increasing in the applied current will lead to the hydraulic engine mount with one notch and one peak frequency like a conventional hydraulic engine mount (in this condition the inner mount will be ineffectual).

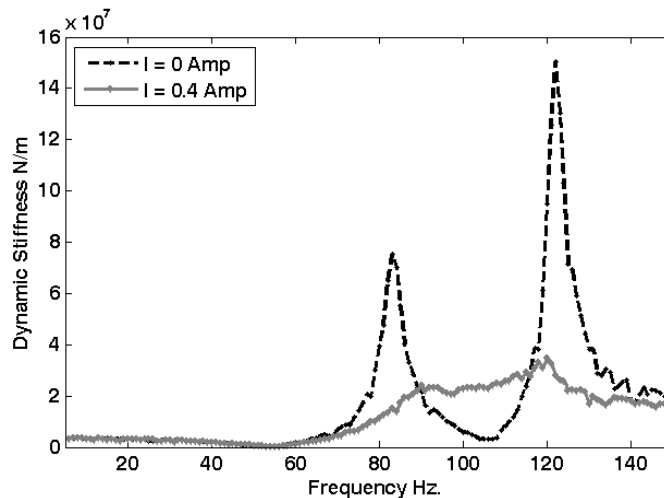


Fig. 13. Dynamic stiffness of the hydraulic engine mount in the ON and OFF states

It must be mentioned that decrease of the peak values of the dynamic stiffness is achieved at the expense of increase of the values of dynamic stiffness between two peaks. By applying magnetic field, in the present of inputs at the peak frequencies, the transmitted force can be reduced effectively.

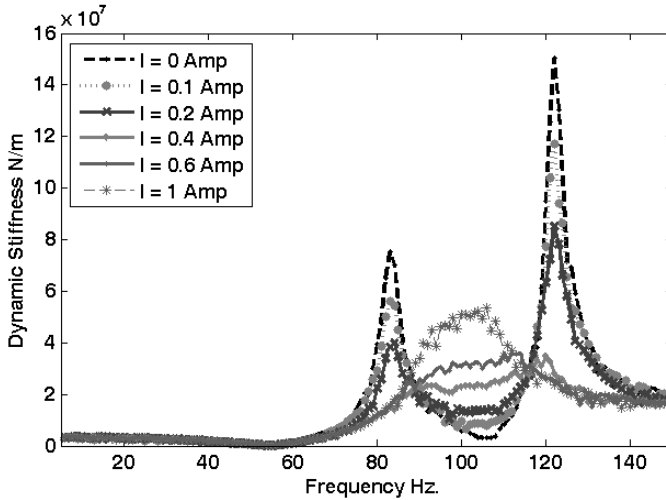


Fig. 14. Effect of magnetic field change on the dynamic stiffness of the proposed hydraulic engine mount

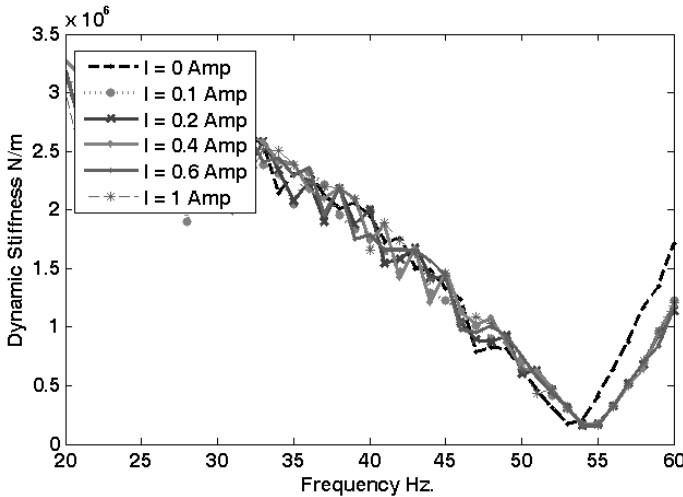


Fig. 15. Independency of the first notch frequency location and depth to the applied magnetic field

Simulation results indicate that by using a magneto-rheological controllable fluid and our proposed hydraulic engine mount design it is possible to effectively isolate the cabin from the engine vibration at the notch frequency and eliminate the peak frequency or change its location by increasing the applied magnetic field.

Conclusions

The paper described a new hydraulic engine mount design that uses two working fluids, one being a controllable fluid. This new design has two notch frequencies and two peak frequencies

and one can put the notch and the peak frequencies to the required locations by changing hydraulic mount parameters. By changing the flow loss of the fluid in the inner inertia track, using a controllable fluid (magneto-rheological fluid), a hydraulic engine mount design with only one notch frequency but no peak frequency is obtained. The main contribution of this study is the elimination of the peak frequency in the new hydraulic engine mount design.

References

- [1] **Yu Y., Peelamedu S. M., Naganathan N. G., Dukkipati R. V.** Automotive vehicle engine mounting systems: a survey. *Journal of Dynamic Systems, Measurement and Control*, Vol. 123, 2001, p. 186-194.
- [2] **Golnaraghi M. F., G. N. Jazar** Development and analysis of a simplified nonlinear model of a hydraulic engine mount. *Journal of Vibration and Control*, Vol. 7, Issue 4, 2001, p. 495-526.
- [3] **Jazar G. N., M. F. Golnaraghi** Nonlinear modeling, experimental verification, and theoretical analysis of a hydraulic engine mount. *Journal of Vibration and Control*, Vol. 8, Issue 1, 2002, p. 87-116.
- [4] **Vahdati N.** A detailed mechanical model of a double pumper fluid mount. *Journal of Vibration and Acoustics, Transactions of the ASME*, Vol. 120, Issue 2, 1998, p. 361-370.
- [5] **Ahmadian M., Y. K. Ahn** Performance analysis of magneto-rheological mounts. *Journal of Intelligent Material Systems and Structures*, Vol. 10, Issue 3, 1999, p. 248-256.
- [6] **Lee B. H., C. W. Lee** Model based feed-forward control of electromagnetic type active control engine-mount system. *Journal of Sound and Vibration*, Vol. 323, Issue3-5, 2009, p. 574-593.
- [7] **Lee Y. W., C. W. Lee** Dynamic analysis and control of an active engine mount system. *Proceedings of the Institution of Mechanical Engineers, Part D: Journal of Automobile Engineering*, Vol. 216, Issue 11, 2002, p. 921-931.
- [8] **Nguyen T., Ciocanel C., Elahinia M.** Analytical modeling and experimental validation of a magnetorheological mount. In *Active and Passive Smart Structures and Integrated Systems 2009*, 2009, San Diego, CA.
- [9] **Baklanov V.** Role of structure noise for new airplane generation. *Journal of Vibroengineering*, Vol. 11, Issue 3, 2009, p. 434-442.
- [10] **Vahdati N.** Double-notch single-pumper fluid mounts. *Journal of Sound and Vibration*, Vol. 285, 2005, p. 697-710.
- [11] **Tikani R., Vahdati N., Ziaei-Rad S., Esfahanian M.** A new hydraulic engine mount design without the peak frequency. *Journal of Vibration and Control*, Vol. 17, Issue 11, 2011, p. 1644-1656.
- [12] **Wood R. L., K. L. Lawrence** Modeling and Simulation of Dynamic Systems. University of Texas at Arlington, 1997.
- [13] **Vahdati N., M. Ahmadian** Variable volumetric stiffness fluid mount design. *Shock and Vibration*, Vol. 11, Issue 1, 2004, p. 21-32.
- [14] **Carlson J. D., D. M. Catanzarite, K. A. St. Clair** Commercial magneto-rheological fluid devices. *International Journal of Modern Physics B*, Vol. 10, 1996, p. 2857-2865.
- [15] **Barber D. E., J. D. Carlson** Performance characteristics of prototype MR engine mounts containing glycol MR fluids. *Journal of Intelligent Material Systems and Structures*, Vol. 21, Issue 15, 2010, p. 1509-1516.
- [16] **Cogdell J. R.** Foundations of Electric Power. New Jersey, 1999.